JACS
JOURNAL OF THE AMERICAN CHEMICAL SOCIETY
Article
pubs.acs.org/JACS

Molecular Motion, Dielectric Response, and Phase Transition of Charge-Transfer Crystals: Acquired Dynamic and Dielectric Properties of Polar Molecules in Crystals

Jun Harada,*[,†,‡] Masaki Ohtani,[‡] Yukihiro Takahashi,[†,‡] and Tamotsu Inabe*[,†,‡]

[†]Department of Chemistry, Faculty of Science, and [‡]Graduate School of Chemical Sciences and Engineering, Hokkaido University, Sapporo 060-0810, Japan

Supporting Information

ABSTRACT: Molecules in crystals often suffer from severe limitations on their dynamic processes, especially on those involving large structural changes. Crystalline compounds, therefore, usually fail to realize their potential as dielectric materials even when they have large dipole moments. To enable polar molecules to undergo dynamic processes and to provide their crystals with dielectric properties, weakly bound charge-transfer (CT) complex crystals have been exploited as a molecular architecture where the constituent polar molecules have some freedom of dynamic processes, which contribute to the dielectric properties of the crystals. Several CT crystals of polar tetrabromophthalic anhydride (TBPA) molecules were prepared using TBPA as an electron acceptor and aromatic hydrocarbons, such as coronene and perylene, as electron donors. The crystal structures and dielectric properties of the CT crystals as well as the single-component crystal of TBPA were investigated at various temperatures. Molecular reorientation of TBPA molecules did not occur in the single-component crystal, and the crystal did not show a dielectric response due to orientational polarization. We have found that the CT crystal formation provides a simple and versatile method to develop molecular dielectrics, revealing that the molecular dynamics of the TBPA molecules and the dielectric property of their crystals were greatly changed in CT crystals. The TBPA molecules underwent rapid in-plane reorientations in their CT crystals, which exhibited marked dielectric responses arising from the molecular motion. An order−disorder phase transition was observed for one of the CT crystals, which resulted in an abrupt change in the dielectric constant at the transition temperature.

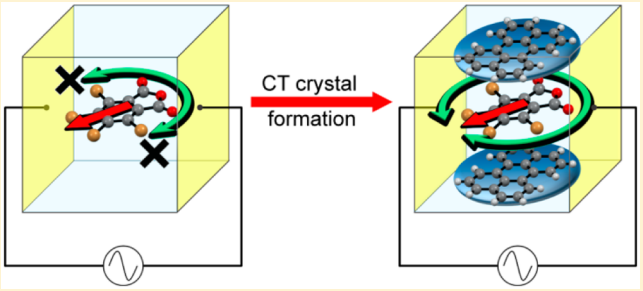

INTRODUCTION

Molecular motion in crystals has been studied in various fields of chemistry.[1] If a molecule does not largely change its structure in the course of a molecular motion, the process is not disturbed by the surrounding molecules and proceeds easily even in crystals. The accumulated information and understanding about the relationship between molecular motions and crystalline environments have paved the way for controlling the molecular dynamics in crystals by designing molecules and crystal structures. Remarkable achievements in the design of crystalline molecules include the realization of molecular machinery that has some analogy with macroscopic objects such as gyroscopes, gears, and bearings.[2] Also of growing interest are macroscopic functions of materials related to molecular motions in crystals. Flipping motion of fluoro-substituted phenyl groups in crystals has been utilized to create dielectric and ferroelectric properties of the materials.[3] Molecular motions of small organic cations such as pyridinium or imidazolium ions also gave rise to ferroelectric properties.[4] However, only limited variations of molecules and molecular motions have been explored, aiming for the development of functional materials with the desired properties. In this paper we describe the design of crystalline materials and control of their molecular-motion-based dielectric properties by incorporating polar molecules into crystalline environments with motional freedom.

Dielectric materials are electrical insulators that can be electrically polarized under an applied electric field. In addition to being of fundamental scientific interest, they are of great value with a variety of applications as basic components of electronic devices, and some of them show piezoelectric, pyroelectric, and ferroelectric properties.[5] Dielectric materials can be characterized by their dielectric constant (electric permittivity) ε^* ($\varepsilon^* = \varepsilon' - i\varepsilon''$, where ε' and ε'' are the real and imaginary parts of the complex dielectric constant, respectively). Molecular motion and reorientation of polar molecules can contribute to the dielectric property of materials in terms of alignment of their permanent dipoles in response to the applied electric field. Compounds of molecules with large dipole moments, therefore, exhibit large dielectric constants in the liquid phase. In the solid state, however, the restriction of the molecular motions severely limits the contribution of orientational polarization. The dielectric constants of materials,

Received: January 14, 2015
Published: March 17, 2015

DOI: 10.1021/jacs.5b00412
J. Am. Chem. Soc. 2015, 137, 4477−4486

consequently, tend to exhibit drastic reduction on solidification.[6] To obtain crystalline materials with large dielectric constants based on molecular motions, it is, therefore, necessary to establish a design guide of crystal structures where molecules with large dipole moments can reorient and respond to the external electric field. Appropriate strategies of crystal engineering combined with designing suitable polar molecules will also be an important step toward the design of ferroelectric molecular crystals, which is a rapidly progressing and promising field of materials science.[7]

We will present a simple and versatile strategy, i.e., formation of weakly bound charge-transfer (CT) complex crystals, to provide planar polar molecules with the ability to reorient in crystals and to respond to the external electric field. CT complexes are formed by attractive intermolecular forces between molecules, where a fraction of electronic charge is transferred from electron-rich donor molecules to electron-poor acceptor molecules. The crystals of CT complexes are of great interest and importance in the field of molecular materials science, showing high electric conductivity,[8] superconductivity,[9] ferroelectricity,[10] and unique magnetic properties.[11] These properties of CT crystals originate from the molecules with partially occupied molecular orbitals produced by the charge transfer. Most of the unique features and functions of CT crystals, therefore, have been limited to those composed of strong donors and/or acceptors, where the degree of charge transfer between the components is large. The CT crystals between weak donors and acceptors, on the other hand, are not expected to display attractive electric properties because both donors and acceptors are electrically neutral in the ground state and their electronic states are almost identical to the ones in the single-component crystals. We have exploited the weak CT crystals as a framework in which polar planar molecules can reorient and respond to the external electric field.

Planar disklike molecules, such as naphthalene and pyrene, often undergo in-plane reorientation in crystals.[1b,12] The reorientation of these molecules is also feasible in their CT crystals, where the aromatics, working as donors, form CT complexes with acceptors such as tetracyanobenzene, tetracyanoethylene, and pyromellitic dianhydride.[13] Solid-state NMR spectroscopic study combined with packing energy calculation by Fyfe and co-workers revealed that naphthalene and pyrene exhibited complete reorientation in the CT crystals. The CT crystals of the rotating molecules often undergo phase transitions at low temperatures, which are related to the order−disorder behavior of molecular orientations of the rotating donors in the crystals.[14] Although the molecular dynamics in some of the CT crystals has been studied intensively, the dynamic nature of the molecules has not been employed for designing functional materials. In this study we have utilized CT crystals as an architecture where polar molecules, which are stationary in their single-component crystals, undergo in-plane reorientation and exhibit dielectric responses to the external electric field (Scheme 1).

We have investigated the crystal structures and dielectric properties of tetrabromophthalic anhydride (TBPA) (**1**) and its CT complexes hexamethylbenzene−TBPA (**2**), coronene−TBPA (**3**), and perylene−TBPA (**4**). The polar electron-accepting molecule TBPA (μ = 4.5 D calculated at the MP2/6-31+G* level) did not show reorientation in the single-component crystals and in the CT crystal with a small donor molecule (**2**), where the TBPA molecule at each crystal site takes only one orientation. In stark contrast, in the CT crystals

Scheme 1. Motional Restriction of Polar Molecules in the Single-Component Crystals and Motional Freedom in CT Crystals[a]

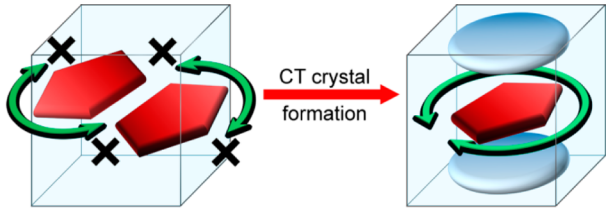

[a]Red pentagons represent the polar molecule, and blue disks represent the other component in CT crystals.

with larger donors (**3** and **4**), TBPA acquired the freedom of reorientation in the crystalline environment and underwent in-plane reorientation, which gave rise to dielectric responses. The crystal of **4** showed a phase transition related to the ordering of dipolar molecules, which induced significant changes in the dielectric constants at the transition temperature. Pretransitional crystal structural changes and the corresponding dielectric responses were also observed and can be interpreted in terms of a slight difference in the potential energies corresponding to the two orientations induced by the breaking of the symmetry of the crystal structure at the phase transition.

EXPERIMENTAL SECTION

Materials. TBPA (**1**), hexamethylbenzene, coronene, and perylene were purchased from Tokyo Chemical Industry. Compound **1** and perylene were purified by vacuum sublimation before crystal growth, while hexamethylbenzene and coronene were used without further purification. Colorless single crystals of **1** were prepared by slow evaporation of benzene solution. Single crystals of CT complexes **2**, **3**, and **4** (**2**, yellow; **3**, orange; **4**, red) were grown from an equimolar benzene solution of **1** and hexamethylbenzene, coronene, or perylene by slow evaporation. Diffuse reflectance spectra of crystalline powders of **2**−**4** clearly show CT bands in the longer wavelength region (Supporting Information).

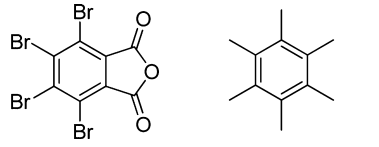

hexamethylbenzene

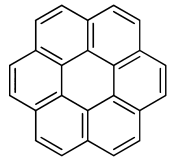
coronene

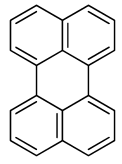
perylene

Single-Crystal X-ray Diffraction Analysis. All of the diffraction measurements were performed on a Bruker SMART APEX II ULTRA diffractometer with a TXS rotating anode (Mo Kα radiation, λ = 0.71073 Å) and multilayer optics. The data collection was carried out using a Japan Thermal Engineering DX-CS190LD N_2-gas-flow cryostat. The temperature in the nozzle was held constant within ±0.2 K during the measurement. The temperature at the sample position was calibrated using a thermocouple, and the calibration was verified by checking the phase transition temperatures, including that of the potassium dihydrogen phosphate (KDP) crystal (123 K).[15] The structures were solved by direct methods (SHELXT-2014) and refined

DOI: 10.1021/jacs.5b00412
J. Am. Chem. Soc. 2015, 137, 4477−4486

Table 1. Crystal Data and Structure Refinement Information for 1−3

	TBPA (1)		hexamethylbenzene−TBPA (2)		coronene−TBPA (3)	
molecular formula	$C_8O_3Br_4$		$C_{20}H_{18}O_3Br_4$		$C_{32}H_{12}O_3Br_4$	
fw	463.72		625.98		764.06	
cryst syst	monoclinic		monoclinic		monoclinic	
space group	$P2_1/n$		$P2_1/m$		$P2_1/c$	
temp (K)	300	100	300	100	300	100
a (Å)	12.6749(10)	12.5164(9)	9.1304(8)	9.0493(7)	7.9540(7)	7.8361(5)
b (Å)	6.1713(5)	6.0894(4)	13.7261(12)	13.3796(10)	9.5826(8)	9.6699(7)
c (Å)	13.4149(11)	13.3977(10)	9.4089(8)	9.3465(7)	16.2147(14)	15.7801(11)
β (deg)	90.8147(12)	90.1220(11)	118.5970(11)	118.3590(9)	89.1480(10)	90.2420(10)
V (Å^3)	1049.22(15)	1021.14(13)	1035.32(16)	995.83(13)	1235.75(18)	1195.72(14)
Z	4	4	2	2	2	2
no. of reflns collected	14615	14161	15274	14633	17910	17195
no. of independent reflns	2379	2320	2464	2366	2866	2751
R_{int}	0.0348	0.0287	0.0260	0.0202	0.0249	0.0220
no. of data/restraints/params	2379/0/137	2320/0/136	2464/0/148	2366/0/148	2866/307/306	2751/0/208
goodness-of-fit on F^2	1.040	1.136	1.038	1.076	1.039	1.047
$R[F^2 > 2\sigma(F^2)]$	0.0214	0.0173	0.0264	0.0150	0.0404	0.0184
$R_w(F^2)$ (all data)	0.0547	0.0426	0.0651	0.0396	0.1173	0.0484

Table 2. Crystal Data and Structure Refinement Information for Perylene−TBPA (4)

molecular formula	$C_{28}H_{12}O_3Br_4$				
fw	716.02				
phase	HTP		LTP		
cryst syst	triclinic		triclinic		
space group	$P\bar{1}$		$P\bar{1}$		
temp (K)	300	265	240	200	100
a (Å)	7.7233(3)	10.0091(8)	9.9896(9)	9.9647(8)	9.9226(8)
b (Å)	9.1834(3)	10.0755(8)	10.0635(9)	10.0419(9)	9.9944(8)
c (Å)	9.1909(3)	12.5454(10)	12.5388(11)	12.5208(11)	12.4828(10)
α (deg)	66.7020(10)	85.0856(13)	85.3160(10)	85.4641(13)	85.7400(11)
β (deg)	84.4390(10)	73.6923(12)	73.8500(10)	73.8886(12)	73.8330(11)
γ (deg)	73.0640(10)	69.0129(12)	69.0270(10)	68.9570(12)	68.8150(11)
V (Å^3)	572.63(3)	1133.55(16)	1130.35(17)	1123.11(17)	1108.14(15)
Z	1	2	2	2	2
no. of reflns collected	11086	21564	21725	21609	21129
no. of independent reflns	2586	5118	5165	5150	5053
R_{int}	0.0287	0.0334	0.0295	0.0292	0.0253
no. of data/restraints/params	2586/123/188	5118/142/299	5165/0/277	5150/0/316	5053/0/316
goodness-of-fit on F^2	1.090	1.065	1.033	1.055	1.070
$R[F^2 > 2\sigma(F^2)]$	0.0494	0.0318	0.0278	0.0220	0.0187
$R_w(F^2)$ (all data)	0.1558	0.0912	0.0765	0.0579	0.0484

by full-matrix least-squares on F^2 using SHELXL-2014.[16] All H atoms were refined using riding models. For the crystal structures without disorders, all non-H atoms were refined anisotropically. For the crystal structures with disorders, details of the refinement were deposited in the Supporting Information as CIFs embedding the SHELXL-2014 res files. The crystal and experimental data are summarized in Tables 1 and 2.

Measurements. The real and imaginary parts of the dielectric constant were measured with an Agilent E4980A precision LCR meter in the frequency range from 500 Hz to 2 MHz. A homemade cryostat was used to control the temperature of the samples under a helium atmosphere between 120 and 360 K. The temperature was measured using a Si diode thermometer mounted on the sample holder. Single crystals of **1**, **2**, and **4** and a compaction pellet of **3** were used as the samples with painted gold paste as the electrodes. Differential scanning calorimetry (DSC) was recorded using a Rigaku Thermo Plus DSC8230 with a heating and cooling rate of 10 K/min to examine the phase transitions of the materials. Diffuse UV−vis reflectance spectra were measured on a Jasco V-570 spectrometer equipped with an integrating sphere accessory (ILN-472). A KBr powder was used as the diluent and the reference. Powder X-ray diffraction patterns were measured using a Bruker D8 ADVANCE and confirmed that the microcrystalline powders used for DSC and dielectric measurements had crystal structures identical to those obtained by single-crystal X-ray diffraction analyses.

RESULTS AND DISCUSSION

Crystal Structure and Dielectric Property of TBPA (1). The orientation of TBPA molecules is ordered in their single-component crystals, which did not show the dielectric response expected for dipolar reorientation. Crystal structure analysis of **1** was carried out at 300 and 100 K. The observed structures were essentially identical to the reported one at room temperature.[17] The nearly planar disklike molecules took only one orientation at each crystal site, and no orientational disorder was detected at both temperatures (Figure 1). The ordered structure indicates that the molecular reorientation of TBPA is not allowed in the crystal. As for the dielectric

DOI: 10.1021/jacs.5b00412
J. Am. Chem. Soc. 2015, 137, 4477−4486

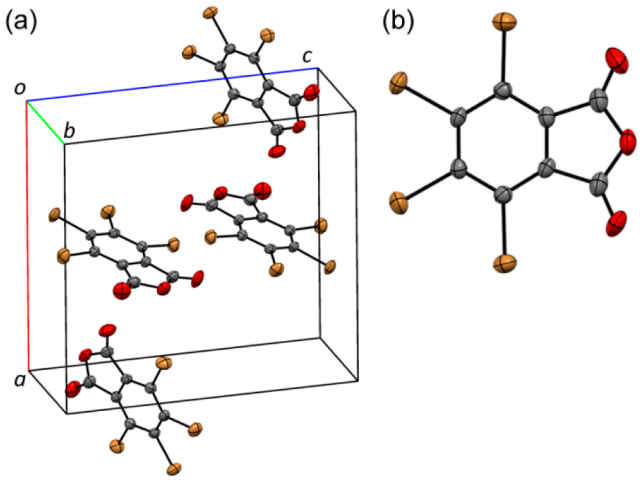

Figure 1. (a) Crystal and (b) molecular structures of TBPA (**1**) at 300 K. The ellipsoids are drawn at the 50% probability level.

property of **1**, neither the real nor imaginary part of the dielectric constant showed significant variation with temperature between 340 and 140 K (Supporting Information). The observed low and temperature-independent dielectric constant ($\varepsilon \approx 5$) clearly shows that, in spite of the large dipole moment of TBPA molecules, they do not contribute to the dielectric properties of the crystal in terms of orientational polarization because they cannot change their orientations in the crystal.

Crystal Structures of Hexamethylbenezene–TBPA (2) and Coronene–TBPA (3). The TBPA molecules were incorporated into CT complex crystals as acceptor molecules with hexamethylbenzene or coronene as donor molecules. Both aromatic donors have round-shaped structures and undergo in-plane rotations in their single-component crystals.[18] While the CT crystals of hexamethylbenzene–TBPA (**2**) did not exhibit orientational disorders of the TBPA molecule, the TBPA molecule in coronene–TBPA (**3**) showed orientational disorder and its temperature dependence. Crystal structures of **2** and **3** were determined at 300 and 100 K. Neither of them showed phase transitions between the temperatures. Both of the CT crystals **2** and **3** were composed of a 1:1 mixture of the donor and acceptor molecules and took a mixed-stack architecture, where the acceptor and donor molecules are stacked alternately to form one-dimensional columns (Figure 2).

In the crystal **2**, the donor molecule hexamethylbenzene lies on a crystallographic center of inversion, and the atoms of the acceptor TBPA molecule reside on a mirror plane. Although the hydrogen atoms of the methyl groups of hexamethylbenzene showed rotational disorder, no other disorder was not detected, and the TBPA molecule took only one orientation. The small values of the dielectric constant of the crystal **2** and its temperature independence confirmed that the orientational motion of the polar TBPA molecule did not take place in the CT crystal **2** (Supporting Information).

In the crystal **3**, both coronene and TBPA molecules reside on centers of inversion. Both the molecules were orientationally disordered at 300 K. The coronene molecule was refined by using the model where the molecule with approximate C_6 symmetry took three different orientations, and the site occupation factors of the three orientations (A, B, C) were refined to be 0.598(9), 0.238(10), and 0.164(9) at 300 K (Figure 3a).

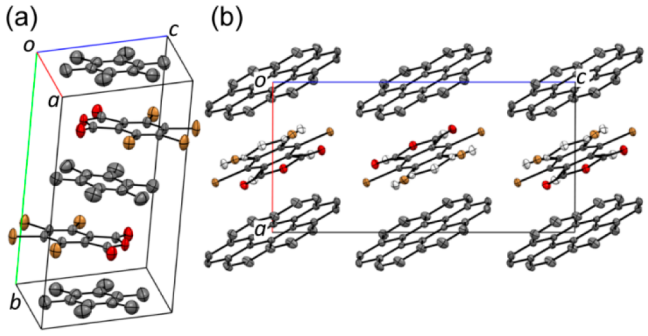

Figure 2. Perspective views of the crystal structures of hexamethylbenzene–TBPA (**2**) and coronene–TBPA (**3**). The ellipsoids are drawn at the 50% probability level. Hydrogen atoms are omitted for clarity. (a) Projection of **2** at 300 K. (b) Projection of **3** at 100 K along the *b* axis. The atoms of one of the two disordered orientations of TBPA are depicted in white.

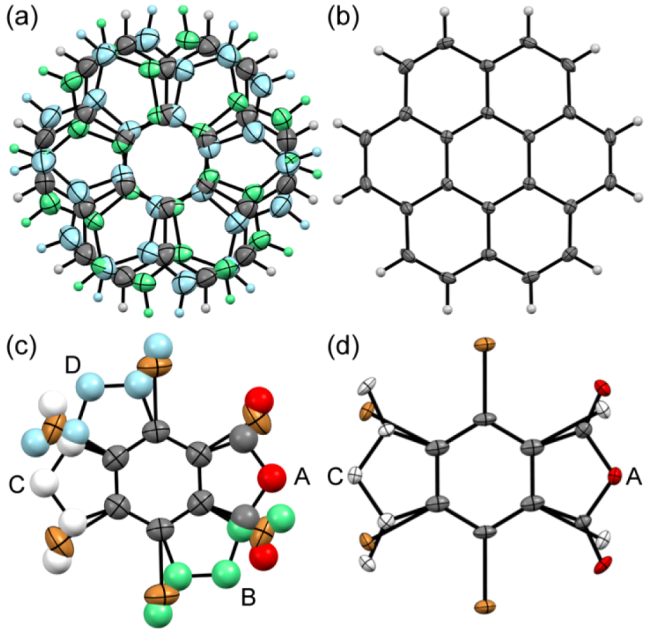

Figure 3. Molecular structures of coronene–TBPA (**3**). The ellipsoids are drawn at the 50% probability level. (a) Coronene molecules at 300 K. The atoms of orientations A, B, and C are depicted in gray, green, and blue, respectively. (b) Coronene molecule at 100 K. (c) TBPA molecules at 300 K. The atoms of the anhydride group (O=C–O–C=O) of orientations B, C, and D are depicted in green, white, and blue, respectively. (d) TBPA molecules at 100 K. The atoms of orientation C are depicted in white.

The disorder of the coronene molecule disappeared at 100 K (Figure 3b), and only one orientation was observed, which shows that the disorder of coronene is dynamic and is caused by in-plane reorientation. The TBPA molecules were also orientationally disordered, and each molecule took four different orientations (A, B, C, and D) at 300 K (Figure 3c). The four orientations can be related to one another by the rotation around the axis that is perpendicular to the molecular plane and passing through the center of the benzene ring. Each of two orientations A and B has its crystallographically equivalent one, i.e., orientations C and D, respectively. Thus, the orientational disorder of TBPA molecules enables the noncentrosymmetric molecule to reside on a center of inversion. The ratio of the populations of orientations A and

DOI: 10.1021/jacs.5b00412
J. Am. Chem. Soc. 2015, 137, 4477–4486

B, which equals that of C and D, was refined to be 0.356:0.144(2) at 300 K. At 100 K the two minor orientations (B and D) disappeared, and only two orientations (A and C) were observed (Figure 3d). The results show that TBPA molecules undergo molecular reorientation and that each of two pairs of orientations (A−B and C−D) equilibrates through a 60° jump in orientation. As for the interconversion of TBPA molecules between orientations A and C or B and D, which can take place through 180° in-plane rotation, neither the crystallographic study nor the dielectric measurements shown in the next section can definitely determine whether it occurs in the crystal **3**, although its occurrence in the crystal **4** was confirmed by both methodologies (see below).

Dielectric Properties of 3. Dielectric responses due to molecular reorientation of TBPA were observed for the crystal of **3**. Figure 4 shows the dielectric constant of **3** measured at several frequencies as a function of temperature. Both the real (ε') and imaginary (ε'') parts of the complex dielectric constant exhibited marked changes with temperature above 150 K, and the changes were dependent on the frequency of the applied electric field. These features of dielectric responses are characteristic of reorientational motion of polar molecules in crystals and can be explained in terms of dielectric relaxation of the molecular dipoles.[6,19]

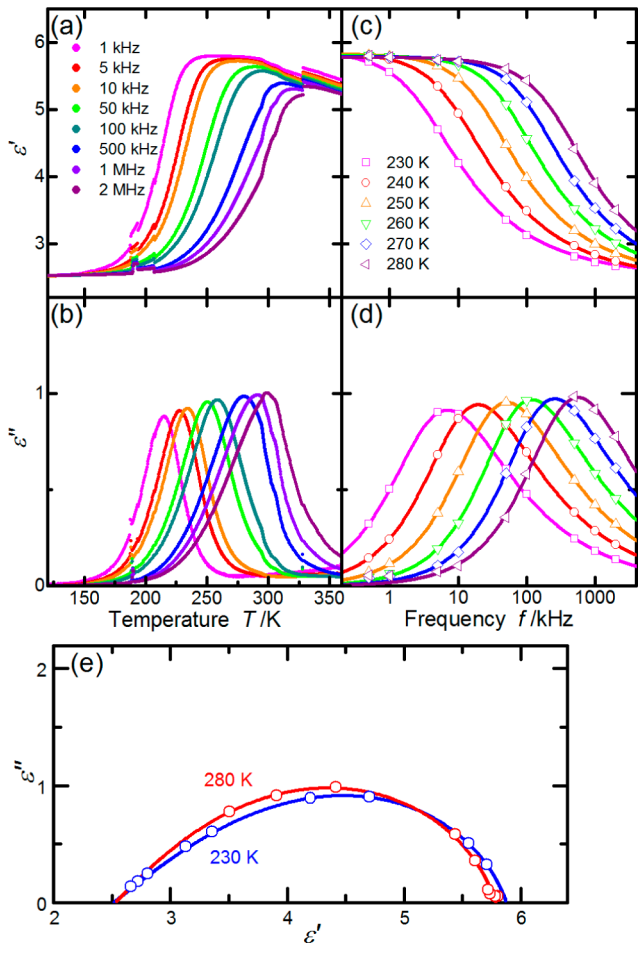

Figure 4. Dielectric properties of coronene−TBPA (**3**). Temperature dependence of (a) the real part (ε') and (b) the imaginary part (ε'') of the complex dielectric constant measured at various frequencies. Frequency dependence of (c) the real part (ε') and (d) the imaginary part (ε'') at several selected temperatures. (e) Relationship between ε' and ε'' (the Cole−Cole diagram). Solid curves in (c)−(e) represent the fit of the experimental data to the Havriliak−Negami model.

In general, rotation of the permanent dipole of polar molecules contributes to the dielectric constant on the condition that the molecules can reorient fast enough to align their dipoles in response to the applied alternating electric field. At low field frequencies, where the molecular reorientation is faster than the reversals of the electric field, the molecular dipoles can follow the switching of the electric field and fully contribute to the dielectric constant, which is observed to have large values. In the high frequency region, where the molecular motion is too slow to follow the electric field, the molecular dipoles are regarded as stationary on the time scale of the ac field and do not contribute to the dielectric constant, which should have small values in the region. In the intermediate frequency region, where the frequencies of the applied field and molecular reorientation are comparable, the molecular dipoles contribute to the dielectric constant with a phase lag between the applied electric field and the induced orientational polarization. The phase lag results in the absorption of energy of the applied electric field by the material, which is known as dielectric loss. The dielectric loss is observed as peaks in the plot of the imaginary part (ε'') against frequency, and the relaxation time of the reorientational motion at that temperature can be derived from the plot. The dielectric loss is negligible in the high and low frequency limits. The ε' values in the intermediate frequency region gradually decrease from a large value at the low frequency limit to a small value at the high frequency limit. In the case of the crystal of **3**, the observed dielectric responses are attributable to the reorientation of polar TBPA molecules, and the reorientation of nonpolar coronene molecules does not contribute to the orientational polarization. The reorientation of TBPA molecules was much slower than the applied frequencies below about 150 K and became much faster around 350 K (Figure 4a). In the intermediate temperature region, the real part increased with temperature and the imaginary part exhibited absorption peaks (Figure 4b), both of which were dependent on the frequency of the ac field.

For more quantitative analysis, the real and imaginary parts of the complex dielectric constant of **3** were plotted against the frequency of the electric field at several selected temperatures (Figure 4c,d). The Cole−Cole diagrams (ε'' vs ε') at two selected temperatures are also shown in Figure 4e. The Cole−Cole plots for **3** deviate from the semicircles or circular arcs expected from the Debye and Cole−Cole relaxation functions, respectively.[20] The skewed circular arcs were well described by the phenomenological relaxation function known as the Havriliak−Negami equation:[21]

$$\varepsilon^*(\omega) = \varepsilon_\infty + \frac{\varepsilon_0 - \varepsilon_\infty}{[1 + (i\omega\tau)^{1-\alpha}]^\beta} \quad (1)$$

where ε^* is the complex dielectric constant, ε_0 and ε_∞ are the low and high frequency limits of the real part of ε^*, respectively ($\varepsilon_0 > \varepsilon_\infty$), τ represents the relaxation time, and ω is equal to 2π times the frequency. The parameters α and β ($0 \le \alpha, \beta \le 1$) are related to the distribution of relaxation times. The Debye ($\alpha = 0$, $\beta = 1$, a semicircle plot) and the Cole−Cole ($0 < \alpha < 1$, $\beta = 1$, a circular arc plot) expressions are special cases of the Havriliak−Negami relation. The parameters for **3** were obtained by fitting the experimental data of the imaginary part (ε'') using eq 1 (Figure 4d). The real parts and the Cole−Cole diagrams of **3** were also well represented by eq 1 using the

DOI: 10.1021/jacs.5b00412
J. Am. Chem. Soc. 2015, 137, 4477−4486

parameters obtained. The relaxation time τ estimated at each temperature followed the Arrhenius equation (eq 2) with good accuracy, which gave an activation energy E_a of 48 kJ/mol for the dielectric relaxation (Figure 5).

$$\tau = C \exp\left(\frac{E_a}{kT}\right) \quad (2)$$

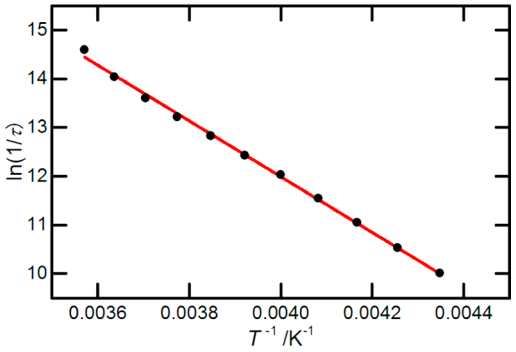

Figure 5. Arrhenius plot of the relaxation time τ as a function of inverse temperature for coronene–TBPA (**3**). The solid line represents the least-squares fit of the data.

The results show that the TBPA molecules, which are stationary in the crystals of **1** and **2**, acquired freedom of reorientation in the CT crystals of **3** with a reasonably small value of the activation energy.[22] As for the mode of reorientation of the TBPA molecules, 60° jump and 180° jump of molecules are not distinguishable from the present dielectric measurements using a compaction pellet of crystalline powders, which lost the information on the anisotropy of the crystal structure and molecular arrangement that can identify the directions of the molecular dipole moments and the course of their changes in the sample.

Crystal Structure and Structural Phase Transition of Perylene–TBPA (4). The CT crystal of perylene–TBPA (**4**) exhibited a structural phase transition related to order–disorder of the orientation of TBPA molecules. The CT crystal **4** consists of a 1:1 mixture of the donor perylene and the acceptor TBPA molecules, which are stacked alternately as the donors and acceptors in the crystals of **2** and **3** (Figure 6a). The crystal **4** belongs to the triclinic $P\bar{1}$ space group at 300 K (high-temperature phase, HTP). Both perylene and TBPA molecules lie on centers of inversion at that temperature, and TBPA is orientationally disordered over two sites with equal occupancies similarly to the TBPA molecule in **3** at 100 K (Figure 6b). As will be shown below, the dielectric measurements confirmed that the disorder of the TBPA molecules was dynamic and originated from a 180° in-plane rotation.

The crystal **4** exhibited a structural phase transition when it was cooled to 100 K. DSC measurement of the microcrystalline sample of **4** showed that the crystals underwent a phase transition at 268 K (Supporting Information). The transition enthalpy ΔH = 1.56 kJ/mol and entropy ΔS = 5.80 J/(K·mol) were calculated from the DSC peak. The magnitude of transition entropy, $\Delta S = R \ln(2.01)$, where R is the gas constant, is consistent with the order–disorder phase transition with two different orientations observed by crystallographic study; see below. X-ray diffraction analysis at 100 K revealed that the cell volume of the crystal **4** was almost doubled in the low-temperature phase (LTP), while the space group ($P\bar{1}$)

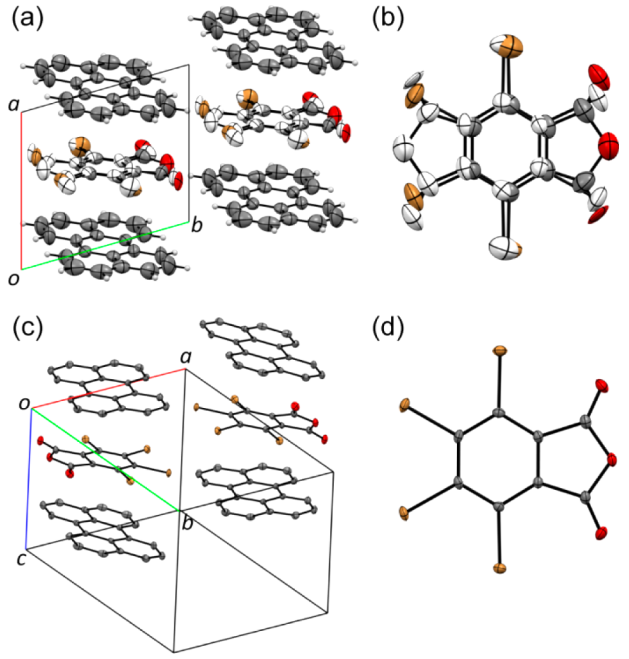

Figure 6. Crystal and molecular structures of perylene–TBPA (**4**). The ellipsoids are drawn at the 50% probability level. Hydrogen atoms in (a) and (c) are omitted for clarity. The atoms of one of the two disordered orientations of TBPA in (a) and (b) are depicted in white. (a) Projection of the crystal structure at 300 K along the *c* axis. The molecules of two unit cells are presented. (b) TBPA molecules at 300 K. (c) Projection of the crystal structure at 100 K along the [1−11] direction. (d) TBPA molecule at 100 K.

remained identical with that in HTP (Table 2, Figure 6a,c). The overall arrangement of molecules in the crystal did not change significantly at this phase transition. In LTP, there are two crystallographically independent perylene molecules in the asymmetric unit and both of them reside on inversion centers. There is a single TBPA molecule in the asymmetric unit, which does not lie on any crystallographic symmetry element. Thus, the orientational disorder of TBPA observed in HTP disappeared at 100 K (Figure 6d), and the phase transition can be defined as the order–disorder type. In the disordered HTP, the polar TBPA molecule is on the inversion center and the dipole moment of each molecule is canceled at each site of the crystal. In the LTP, on the other hand, the TBPA molecule at each site has its polarity. Although the changes in the degrees of order of the orientation and dipole at each site satisfy some of the prerequisites for ferroelectric phase transitions, the centrosymmetry of the crystal (nonpolar space group $P\bar{1}$) in LTP rules out the possibility of ferroelectric transition. On the basis of the observed structure changes, the phase transition of **4** is expected to be a para- to antiferroelectric one.

It should be noted that the orientational disorder of TBPA molecules in **3** and **4** was related to crystallographic symmetry elements and that the appearance and disappearance of the disorder dominated the phase transition of **4**. Although dynamic disorders of molecules often disappear at low temperature, most of them are not related to phase transitions. This is especially the case for orientational disorders of small molecules in clathrate crystals or disorders of only a part of the whole molecule, such as alkyl chains or tertiary butyl groups. Even the orientational disorders of whole molecules are not necessarily related to phase transitions.[23] Introduction of a new

DOI: 10.1021/jacs.5b00412
J. Am. Chem. Soc. 2015, 137, 4477–4486

symmetry element (i.e., an inversion center) by the disorder of TBPA molecules in the CT crystals indicated that the orientational order of the molecules, although it varies with crystals, is not a trivial matter to the crystals and that the order and disorder of the orientation can switch the symmetry of the crystal site between pseudocentrosymmetric and centrosymmetric and toggle the polarity and nonpolarity of the site.

Dielectric Properties of 4. Dielectric measurements of the crystal of **4** confirmed that the TBPA molecules underwent in-plane reorientation in the crystal, and the dielectric properties exhibited marked changes at the order−disorder phase transition. Figure 7 shows the dielectric constant of **4** measured

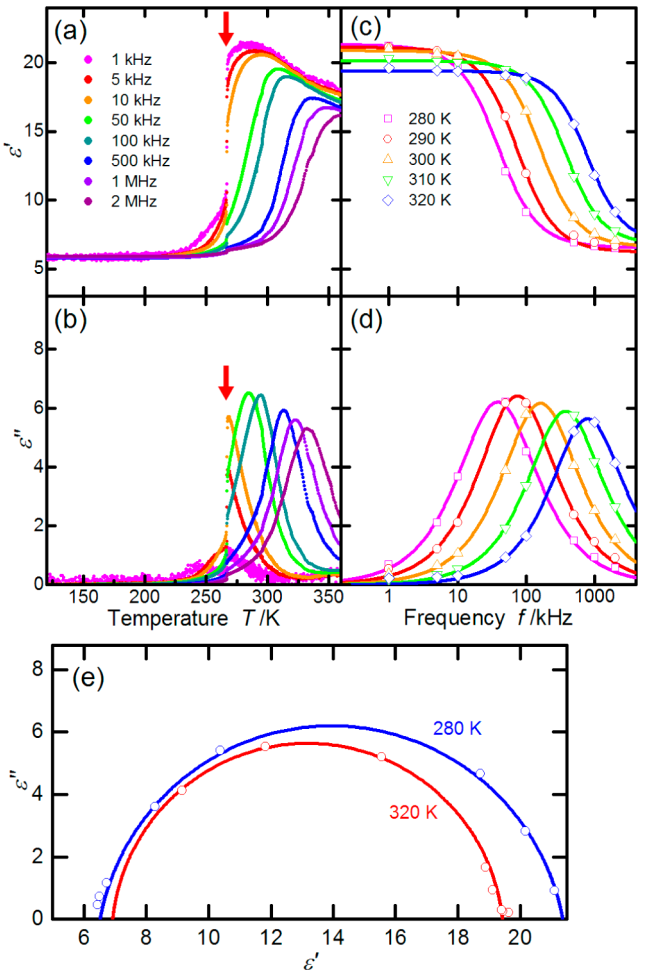

Figure 7. Dielectric properties of perylene−TBPA (**4**). Temperature dependence of (a) the real part (ε') and (b) the imaginary part (ε'') of the complex dielectric constant measured at various frequencies. The phase transition temperature is shown by arrows. Frequency dependence of (c) the real part (ε') and (d) the imaginary part (ε'') at several selected temperatures. (e) Relationship between ε' and ε'' (the Cole−Cole diagram). Solid curves in (c)−(e) represent the fit of the experimental data to the Cole−Cole model.

at several frequencies (1 kHz to 2 MHz) as a function of temperature. The electric field was applied along the crystal *b* axis of the unit cell of HTP, which is parallel to the direction of the dipole moment vector of TBPA molecules in the crystal. In HTP (above around 270 K), both the real (ε') and imaginary (ε'') parts of the dielectric constant showed temperature dependence similar to that observed for **3** (Figure 7a,b). As the temperature was decreased, the dielectric constant abruptly dropped at the transition temperature. The dielectric constant further decreased with lowering of the temperature in LTP. As discussed in the next section, the smaller values of the dielectric constant in LTP in the vicinity of the phase transition temperature reflect a suppressed dielectric response due to the energy difference between the two orientations in the crystal lattice.

The frequency dependence of the complex dielectric constant of **4** in HTP (Figure 7c,d) and the symmetric circular arcs of its Cole−Cole diagram (Figure 7e) were represented well by the Cole−Cole equation (eq 3),[20] which is a special case ($\beta = 1$) of the Havriliak−Negami equation (eq 1).

$$\varepsilon^*(\omega) = \varepsilon_\infty + \frac{\varepsilon_0 - \varepsilon_\infty}{1 + (i\omega\tau)^{1-\alpha}} \quad (3)$$

The Arrhenius fitting of the estimated relaxation time τ yielded the activation energy 56 kJ/mol for the dielectric relaxation (Figure 8). These results clearly show that the TBPA

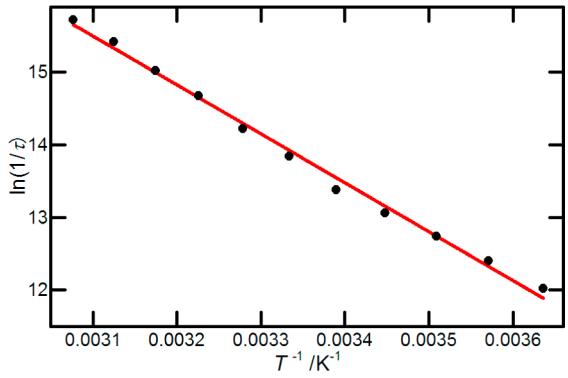

Figure 8. Arrhenius plot of the relaxation time τ as a function of inverse temperature for perylene−TBPA (**4**). The solid line represents the least-squares fit of the data.

molecules of **4** in HTP also exhibited in-plane reorientation and dielectric responses and that the change in the degree of orientational order at low temperature induced a dielectric phase transition.

Pretransitional Crystal Structure Changes and Mechanism of the Order−Disorder Phase Transition of 4. To gain further understanding of the order−disorder phase transition of **4**, we examined the pretransitional behavior of the molecules in the crystal and found that the order−disorder transition was induced by changes not in the molecular dynamics but in the relative stability of the two orientations. X-ray diffraction analysis of **4** in LTP was carried out at several temperatures in the vicinity of the transition temperature. Figure 9 shows the difference electron density maps on the least-squares mean plane of the atoms of the TBPA molecule. At 200 K only one orientation of TBPA was observed, and the map shows no significant residual peaks that can belong to the atoms of the molecule with another orientation (Figure 9a). At 240 K, however, two residual peaks appeared and can be assigned to the two Br atoms of the minor orientation (Figure 9b). The intensities of the peaks increased at 265 K, a few kelvin below the transition temperature, and other peaks of the atoms of the minor orientation were detected at this temperature (Figure 9c). The ratio of the populations of the major and the minor orientations was refined to be 0.9167:0.0833(8) at 265 K.

DOI: 10.1021/jacs.5b00412
J. Am. Chem. Soc. 2015, 137, 4477−4486

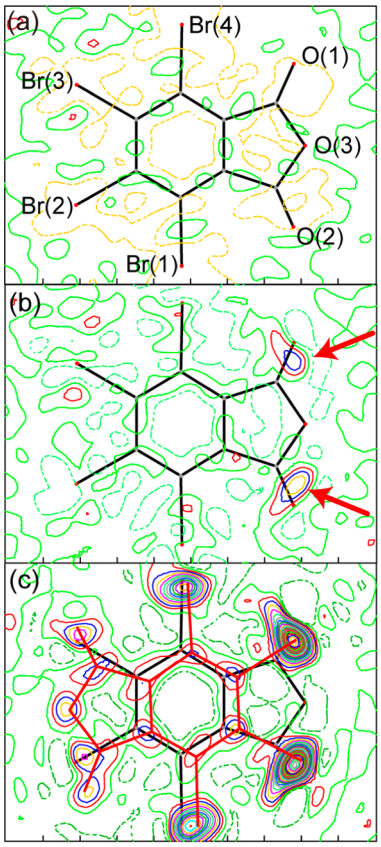

Figure 9. Difference electron density maps of perylene−TBPA (**4**). Each map is the least-squares mean plane of the atoms of the TBPA molecule. The contour lines are at 0.2 e $Å^{-3}$ intervals. Negative contours are indicated by broken lines. (a) At 200 K. (b) At 240 K. The residual peaks corresponding to the atoms of the minor orientation are indicated by arrows. (c) At 265 K. The molecular skeleton of the minor orientation is drawn in red.

These results clearly show that the orientation of the TBPA molecule was not completely ordered in the "ordered" LTP but mostly biased toward one of the two orientations. The disappearance of the minor orientation below 200 K indicates the following: The two orientations were equilibrating with each other through molecular reorientation even in LTP at least near the phase transition temperature, and the amount of the minor orientation decreased to be negligible as the temperature was lowered according to the Boltzmann distribution law. The small but significant dielectric response observed in LTP (Figure 7a,b) is consistent with the occurrence of reorientational motion of TBPA and concomitant dipolar relaxation in LTP.[24]

The observed changes in the crystal structure of **4** between 300 and 100 K are characteristic of order−disorder phase transitions, which tend to be interpreted as follows: In the high-temperature phase, the molecule dynamically changes its orientation between the two crystallographically equivalent ones and the observed structure is therefore disordered. In the low-temperature phase, in contrast, the molecular reorientation is frozen and each molecule is confined to one orientation that corresponds to a minimum of the rotational potential energy surface defined by the crystal lattice. The pretransitional structural changes and the dielectric response of **4**, however, clearly show that the molecular reorientation of TBPA was not frozen in LTP.[26] Only a small difference in the relative stability of two orientations decreases the amount of the minor orientation to be undetectable by X-ray diffraction analysis.[27] Ordered structures in the low-temperature phase at order−disorder transitions are likely to be related to the energy difference between structures responsible for the disorder rather than the freezing of their dynamic exchanges.

Halogen Bonding in the Crystals 1 and 2. The ordered orientation of TBPA molecules in the crystals of **1** and **2** can be rationalized in terms of the preference of one orientation due to intermolecular halogen bonding.[28] Figure 10 illustrates the arrangements of TBPA molecules in the crystals of **1** and **2**.

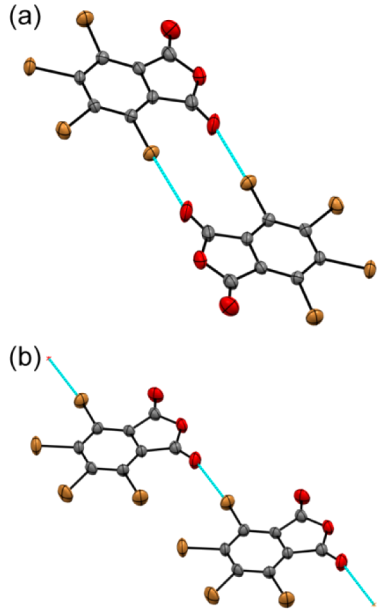

Figure 10. TBPA molecules linked by the C−Br···O halogen bonds in crystals. The ellipsoids are drawn at the 50% probability level. (a) TBPA (**1**) at 300 K. (b) Hexamethylbenzene−TBPA (**2**) at 300 K.

Short and almost linear contacts of (C−)Br···O (**1** at 300 K, 3.1525(26) Å, 175.65(10)°; **2** at 300 K, 2.9993(26) Å, 174.29(11)°) are indicative of halogen bonding,[29] and TBPA molecules in both crystals are connected to the neighboring ones by the halogen bonds. The intermolecular halogen bonding should make the observed orientation energetically much more favorable than the other possible ones. The reorientation of TBPA molecules and dielectric response of the crystals are not allowed because the residence time of molecules at any other disfavored orientations is negligibly short even if the process of molecular reorientation is not inhibited by the surrounding molecules. In contrast, no halogen bonding or other significant intermolecular contact, except CT interactions, was detected in the crystal structures of **3** and **4**, where the TBPA molecules undergo molecular reorientation.

CONCLUSION

We have found that the dynamic nature of TBPA molecules in crystals and their dielectric responses were drastically enhanced by formation of CT crystals and that, despite their static nature in the single-component crystal, the polar molecules acquired dynamic properties in their CT crystals. In the single-component crystal of TBPA (**1**) and the CT crystal with hexamethylbenzene (**2**), each TBPA molecule took only one orientation that was energetically favored due to intermolecular

DOI: 10.1021/jacs.5b00412
J. Am. Chem. Soc. 2015, 137, 4477−4486

halogen bonding, and the crystals did not show any dielectric anomaly. In the CT crystals with coronene (**3**) and perylene (**4**), in contrast, each TBPA molecule was orientationally disordered at room temperature and dynamic exchange between different orientations resulted in marked dielectric responses of the crystals. The changes in the molecular dynamics and orientational order of TBPA molecules are likely to be brought about by additional free space available in the CT crystals and/or centrosymmetric environment of TBPA in the crystals induced by the centrosymmetric donor molecules. The present results tend to show that the larger the donors, the more mobility and freedom of orientation TBPA acquires in the CT crystals.

The present study has demonstrated that formation of weakly bound CT crystals can provide a simple and versatile method to modify the dynamic properties of polar compounds and also a design guide to construct dielectric crystalline materials. Only if a polar molecule of interest has some electron donor or acceptor character is a wide range of choice available for the constituent donor or acceptor molecules to form CT crystals. The formation of CT crystals of polar molecules is, therefore, a promising approach to develop dielectric materials with desired properties, in a way similar to the successful development of organic conductive and superconductive materials.

We have also found that the CT crystal formations tend to impose centrosymmetry or pseudocentrosymmetry on the site of the TPBA molecule, the symmetry of which can be switched with phase transitions. The crystal **4** showed an order−disorder phase transition, where the dielectric property was abruptly changed. The pretransitional changes in the crystal structure were observed, and the transition was interpreted not in terms of freezing of the molecular reorientation but in terms of the energy difference between the two interconverting orientations in the low-temperature phase. Although the crystal structure changes indicate that the transition of **4** belongs to a para- to antiferroelectric one, several features of the transition satisfied some of the conditions required for para- to ferroelectric phase transitions.

In phase transitions of crystalline dielectric materials, the nature of the transitions, such as ferroelectric or antiferroelectric, is mainly determined by the symmetry and polarity of the crystals, regulation of which requires the control of the crystal structures. Although controlling the crystal structures and phase transitions is, in general, not possible at present, the arrangement of molecules in the weakly bound CT crystals is largely predetermined: i.e., the donor and acceptor molecules are alternately stacked to form one-dimensional columns, in which the molecular dipoles stack parallel or antiparallel to each other. Only a limited number of interactions have to be considered to understand the structures and to shift the course of phase transitions of the CT crystals. We are now undertaking a systematic study of the CT crystals of TBPA or its chloro analogue, tetrachlorophthalic anhydride (TCPA), using different aromatic hydrocarbons as donors. DSC and X-ray diffraction studies have revealed that many of them undergo phase transitions below or above room temperature,[31] which has made this class of CT crystals a promising target of exploration. Further investigation of CT crystals of polar molecules with interchangeable donor or acceptor component molecules will serve to significantly advance the development of crystalline dielectric materials.

■ ASSOCIATED CONTENT

Supporting Information

Diffuse reflectance spectra of crystalline powders of **1**−**4**, hexamethylbenzene, coronene, and perylene, temperature dependence of the complex dielectric constants of **1** and **2**, DSC of **4**, and X-ray crystallographic data (CIF). This material is available free of charge via the Internet at http://pubs.acs.org.

■ AUTHOR INFORMATION

Corresponding Authors

*junharada@sci.hokudai.ac.jp
*inabe@sci.hokudai.ac.jp

Notes

The authors declare no competing financial interest.

■ ACKNOWLEDGMENTS

This work was supported in part by a Grant-in-Aid for Scientific Research from the Ministry of Education, Culture, Sports, Science and Technology of Japan. We are grateful to Dr. Kobayashi at Hokkaido University for permission to use the Bruker D8 ADVANCE powder X-ray diffractometer.

■ REFERENCES

(1) (a) Gavezzotti, A.; Simonetta, M. *Chem. Rev.* **1982**, *82*, 1−13. (b) Fyfe, C. A. *Solid State NMR for Chemists*; CFC Press, Guelph, Canada, 1983. (c) *Dynamics of Molecular Crystals. Studies in Physical and Theoretical Chemistry 46*; Lascombe, J., Ed.; Elsevier: Amsterdam, 1987. (d) Gavezzotti, A.; Simonetta, M. In *Organic Solid State Chemistry. Studies in Organic Chemistry 32*; Desiraju, G. R., Ed.; Elsevier: Amsterdam, 1987; Chapter 11. (e) Dunitz, J. D.; Maverick, E. F.; Trueblood, K. N. *Angew. Chem., Int. Ed. Engl.* **1988**, *27*, 880−895. (f) Harris, K. D. M.; Aliev, A. E. *Chem. Br.* **1995**, 132−136. (g) Bürgi, H. B. *Annu. Rev. Phys. Chem.* **2000**, *51*, 275−296. (h) Harada, J.; Ogawa, K. In *Topics in Stereochemistry*; Denmark, S. E., Siegel, J. S., Eds.; John Wiley & Sons, Inc.: 2006; Vol. *25*, p 31. (i) Vogelsberg, C. S.; Garcia-Garibay, M. A. *Chem. Soc. Rev.* **2012**, *41*, 1892−1910.

(2) (a) Garcia-Garibay, M. A. *Proc. Natl. Acad. Sci. U.S.A.* **2005**, *102*, 10771−10776. (b) Karlen, S.; Garcia-Garibay, M. *Top. Curr. Chem.* **2005**, *262*, 179−227. (c) Khuong, T.-A. V.; Nunez, J. E.; Godinez, C. E.; Garcia-Garibay, M. A. *Acc. Chem. Res.* **2006**, *39*, 413−422. (d) Sokolov, A. N.; Swenson, D. C.; MacGillivray, L. R. *Proc. Natl. Acad. Sci. U.S.A.* **2008**, *105*, 1794−1797. (e) Karlen, S. D.; Reyes, H.; Taylor, R. E.; Khan, S. I.; Hawthorne, M. F.; Garcia-Garibay, M. A. *Proc. Natl. Acad. Sci. U.S.A.* **2010**, *107*, 14973−14977. (f) Lemouchi, C.; Mézière, C.; Zorina, L.; Simonov, S.; Rodríguez-Fortea, A.; Canadell, E.; Wzietek, P.; Auban-Senzier, P.; Pasquier, C.; Giamarchi, T.; Garcia-Garibay, M. A.; Batail, P. *J. Am. Chem. Soc.* **2012**, *134*, 7880−7891. (g) Sato, S.; Yamasaki, T.; Isobe, H. *Proc. Natl. Acad. Sci. U.S.A.* **2014**, *111*, 8374−8379.

(3) (a) Horansky, R. D.; Clarke, L. I.; Price, J. C.; Khuong, T.-A. V.; Jarowski, P. D.; Garcia-Garibay, M. A. *Phys. Rev. B: Condens. Matter Mater. Phys.* **2005**, *72*, 014302. (b) Horansky, R. D.; Clarke, L. I.; Winston, E. B.; Price, J. C.; Karlen, S. D.; Jarowski, P. D.; Santillan, R.; Garcia-Garibay, M. A. *Phys. Rev. B: Condens. Matter Mater. Phys.* **2006**, *74*, 054306. (c) Akutagawa, T.; Koshinaka, H.; Sato, D.; Takeda, S.; Noro, S.-I.; Takahashi, H.; Kumai, R.; Tokura, Y.; Nakamura, T. *Nat. Mater.* **2009**, *8*, 342−347.

(4) (a) Czarnecki, P.; Nawrocik, W.; Pająk, Z.; Wąsicki, J. *J. Phys.: Condens. Matter* **1994**, *6*, 4955−4960. (b) Wąsicki, J.; Czarnecki, P.; Pająk, Z.; Nawrocik, W.; Szczepański, W. *J. Chem. Phys.* **1997**, *107*, 576−579. (c) Pająk, Z.; Czarnecki, P.; Szafrańska, B.; Małuszyńska, H.; Fojud, Z. *Phys. Rev. B: Condens. Matter Mater. Phys.* **2004**, *69*, 132102. (d) Przesławski, J.; Kosturek, B.; Dacko, S.; Jakubas, R. *Solid State Commun.* **2007**, *142*, 713−717. (e) Zhang, Y.; Ye, H.-Y.; Cai, H.-L.; Fu, D.-W.; Ye, Q.; Zhang, W.; Zhou, Q.; Wang, J.; Yuan, G.-L.; Xiong, R.-G. *Adv. Mater.* **2014**, *26*, 4515−4520.

DOI: 10.1021/jacs.5b00412
J. Am. Chem. Soc. 2015, 137, 4477−4486

(5) Lines, M. E.; Glass, A. M. *Principles and Applications of Ferroelectrics and Related Materials*; Clarendon Press: Oxford, U.K., 1977.
(6) Wright, J. D. *Molecular Crystals*, 2nd ed.; Cambridge University Press: Cambridge, U.K., 1995.
(7) (a) Horiuchi, S.; Ishii, F.; Kumai, R.; Okimoto, Y.; Tachibana, H.; Nagaosa, N.; Tokura, Y. *Nat. Mater.* **2005**, *4*, 163−166. (b) Horiuchi, S.; Tokura, Y. *Nat. Mater.* **2008**, *7*, 357−366. (c) Horiuchi, S.; Tokunaga, Y.; Giovannetti, G.; Picozzi, S.; Itoh, H.; Shimano, R.; Kumai, R.; Tokura, Y. *Nature* **2010**, *463*, 789−792. (d) Horiuchi, S.; Kagawa, F.; Hatahara, K.; Kobayashi, K.; Kumai, R.; Murakami, Y.; Tokura, Y. *Nat. Commun.* **2012**, *3*, 1308.
(8) (a) Ferraris, J.; Cowan, D. O.; Walatka, V.; Perlstein, J. H. *J. Am. Chem. Soc.* **1973**, *95*, 948−949. (b) Saito, G.; Yoshida, Y. *Bull. Chem. Soc. Jpn.* **2007**, *80*, 1−137.
(9) Jérome, D. *Science* **1991**, *252*, 1509−1514.
(10) (a) Tokura, Y.; Koshihara, S.; Iwasa, Y.; Okamoto, H.; Komatsu, T.; Koda, T.; Iwasawa, N.; Saito, G. *Phys. Rev. Lett.* **1989**, *63*, 2405−2408. (b) Okamoto, H.; Mitani, T.; Tokura, Y.; Koshihara, S.; Komatsu, T.; Iwasa, Y.; Koda, T.; Saito, G. *Phys. Rev. B: Condens. Matter Mater. Phys.* **1991**, *43*, 8224−8232. (c) Kobayashi, K.; Horiuchi, S.; Kumai, R.; Kagawa, F.; Murakami, Y.; Tokura, Y. *Phys. Rev. Lett.* **2012**, *108*, 237601.
(11) (a) Miller, J. S.; Calabrese, J. C.; Rommelmann, H.; Chittipeddi, S. R.; Zhang, J. H.; Reiff, W. M.; Epstein, A. J. *J. Am. Chem. Soc.* **1987**, *109*, 769−781. (b) Miller, J. S. *J. Mater. Chem.* **2010**, *20*, 1846−1857.
(12) Boyd, R. K.; Fyfe, C. A.; Wright, D. A. *J. Phys. Chem. Solids* **1974**, *35*, 1355−1365.
(13) (a) Fyfe, C. A. *J. Chem. Soc., Faraday Trans. 2* **1974**, *70*, 1633−1641. (b) Fyfe, C. A. *J. Chem. Soc., Faraday Trans. 2* **1974**, *70*, 1642−1649. (c) Fyfe, C. A.; Harold-Smith, D.; Ripmeester, J. *J. Chem. Soc., Faraday Trans. 2* **1976**, *72*, 2269−2282.
(14) Herbstein, F. H. *Crystalline Molecular Complexes and Compounds*; Oxford University Press: Oxford, U.K., 2005; Vol. *2*, Chapter 16.
(15) Tomaszewski, P. E. *Phase Transitions* **1992**, *38*, 127−220.
(16) Sheldrick, G. M. *Acta Crystallogr., Sect. A* **2008**, *64*, 112−122.
(17) Sake Gowda, D. S.; Rudman, R. *Acta Crystallogr. Sect. B* **1982**, *38*, 2842−2845.
(18) (a) Allen, P. S.; Cowking, A. *J. Chem. Phys.* **1967**, *47*, 4286−4289. (b) Van Steenwinkel, R. *Z. Naturforsch., A* **1969**, *24*, 1526−1531. (c) Fyfe, C. A.; Dunell, B. A.; Rimeester, J. *Can. J. Chem.* **1971**, *49*, 3332−3335.
(19) Kao, K. C. *Dielectric Phenomena in Solids: With Emphasis on Physical Concepts of Electronic Processes*; Elsevier Academic Press: San Diego, 2004.
(20) Cole, K. S.; Cole, R. H. *J. Chem. Phys.* **1941**, *9*, 341−351.
(21) Havriliak, S.; Negami, S. *Polymer* **1967**, *8*, 161−210.
(22) The activation energies of in-plane reorientation of hexamethylbenzene, coronene, and pyrene in crystals were reported to be 28.1, 25.2, and 60.9 kJ/mol, respectively.[1b]
(23) Harada, J.; Ogawa, K. *Chem. Soc. Rev.* **2009**, *38*, 2244−2252.
(24) The small dielectric response in LTP is consistent with Debye-type orientational polarization.[25] The energy difference in the two orientations without an electric field decreases the number of molecular dipoles that change their orientation in response to the applied electric field.
(25) Debye, P. J. W. *Polar Molecules*; Chemical Catalogue Co.: New York, 1929.
(26) From the Arrhenius relation obtained in Figure 8, the relaxation time τ at the transition temperature is calculated to be 1.1×10^{-5} s^{-1}.
(27) (a) Harada, J.; Ogawa, K. *J. Am. Chem. Soc.* **2001**, *123*, 10884−10888. (b) Harada, J.; Harakawa, M.; Ogawa, K. *CrystEngComm* **2008**, *10*, 1777−1781.
(28) (a) Metrangolo, P.; Resnati, G. *Chem.—Eur. J.* **2001**, *7*, 2511−2519. (b) Desiraju, G. R.; Ho, P. S.; Kloo, L.; Legon, A. C.; Marquardt, R.; Metrangolo, P.; Politzer, P.; Resnati, G.; Rissanen, K. *Pure Appl. Chem.* **2013**, *85*, 1711−1713. (c) Priimagi, A.; Cavallo, G.; Metrangolo, P.; Resnati, G. *Acc. Chem. Res.* **2013**, *46*, 2686−2695. (d) Lemouchi, C.; Vogelsberg, C. S.; Zorina, L.; Simonov, S.; Batail, P.; Brown, S.; Garcia-Garibay, M. A. *J. Am. Chem. Soc.* **2011**, *133*, 6371−6379. (e) Lemouchi, C.; Yamamoto, H. M.; Kato, R.; Simonov, S.; Zorina, L.; Rodríguez-Fortea, A.; Canadell, E.; Wzietek, P.; Iliopoulos, K.; Gindre, D.; Chrysos, M.; Batail, P. *Cryst. Growth Des.* **2014**, *14*, 3375−3383.
(29) The sum of the van der Waals radii of Br and O atoms is 3.37 Å.[30]
(30) Bondi, A. *J. Phys. Chem.* **1964**, *68*, 441−451.
(31) For example, the chloro analogue of **2**, i.e., hexamethylbenzene−TCPA, underwent a phase transition at 401 K. The chloro analogue of **4**, perylene−TCPA, crystallized in two forms, both of which also showed a phase transition (at 233 and 148 K, respectively).

DOI: 10.1021/jacs.5b00412
J. Am. Chem. Soc. 2015, 137, 4477−4486